Design and study of structural linear and nonlinear optical properties of Chiral [Fe(phen)3] 2+ complexes

Ahmad Naïm, Yacine Bouhadja, Miguel Cortijo, Elen Duverger-Nédellec, Howard Flack, Eric Freysz, Philippe Guionneau, Antonio Iazzolino, Amine Ould Hamouda, Patrick Rosa, et al.

HAL Id: hal-01830744
https://hal.science/hal-01830744

Submitted on 5 Dec 2018

Design and study of structural, linear and nonlinear optical properties of chiral [Fe(phen)₃]²⁺ complexes

Ahmad Naim,[a] Yacine Bouhadja,[b] Miguel Cortijo,[a,c] Elen Duverger-Nédellec,[a] Howard D. Flack,[d†] Eric Freysz,[e]* Philippe Guionneau,[a] Antonio Iazzolino,[e] Amine Ould Hamouda,[e] Patrick Rosa,[a]* Olaf Stefańczyk,[a] Ángela Valentín-Pérez[a,c] and Mehdi Zeggar[a,b]

[a] CNRS, Univ. Bordeaux, ICMCB, UMR 5026, F-33600 Pessac, France. [b] Department of Chemistry, University of Annaba, BP 12-23200 Sidi-Ammar, Algérie. [c] CNRS, Univ. Bordeaux, CRPP, UMR 5031, F-33600 Pessac, France. [d] Chimie minérale, analytique et appliquée, Sciences II, Université de Genève, 30, quai Ernest-Ansermet CH-1211 Geneva Switzerland. [e] LOMA, UMR CNRS 5798, 351 Cours de la Libération, FR-33405 Talence Cedex, France.

ABSTRACT: The dependence of non-linear optical properties upon the spin state in molecular switches is still and unexplored area. Chiral [Fe(*phen*)₃]²⁺ complexes are excellent candidates to those studies since they are expected to show non-linear optical properties of interest and at the same time, they show photoconversion to a short-lived metastable High-Spin state by ultrafast optical pumping. Herein we present the synthesis, crystallographic and spectroscopic comparison of chiral [Fe(*phen*)₃]²⁺ complexes obtained with chiral anions, a new lipophilic derivative of the D_2-symmetric (As₂(tartrate)₂)²⁻, and D_3-symmetric TRISCAT, TRISCAS and TRISPHAT. Complexes [Fe(*phen*)₃](*rac*-TRISCAT)₂ (**2**) and [Fe(*phen*)₃](X-TRISCAS)₂ (X = *rac* (**3**), Δ (**4**), Λ (**5**)) were found to be isomorphous in the *R*32 Sohncke space group, with twinning by inversion correlated with the starting chiral anion optical purity. The structures show the [Fe(*phen*)₃]²⁺ complex interacting strongly along its 3-fold axis with two anions. Only the structure of a ([Fe(*phen*)₃](*rac*-TRISPHAT)₂ solvate (**6**) could be obtained, which showed no particular anion/cation interaction, contrary to what observed previously in solution. The [Fe(*phen*)₃](X-As₂(tartrate)₂) (X = Δ (**7**), Λ (**8**), and racemic mixture (**9**)) crystallize in enantiomorphic space groups $P3_121/P3_221$ with the same solid state packing. Dichroic electronic absorption studies evidenced racemization for all chiral complexes in solution due to ion pair dissociation, while the asymmetric induction is conserved in the solid state in KBr pellets. We evidenced on chiral complexes **4** and **5** strong non-linear second harmonic generation, the intensity of which could be correlated with the complex electronic absorption.

Introduction

Photophysical properties of Fe(II) complexes with polyimine ligands, such as [Fe(*bipy*)₃]²⁺, [Fe(*phen*)₃]²⁺, or [Fe(*terpy*)₂]²⁺, where *bipy* = 2,2'-bipyridine, *phen* = 9,10-phenantroline and *terpy* = 2,2':6',2"-terpyridine, have been the subject of intense scrutiny recently.[1–6] These studies are of course of fundamental interest for the understanding of photophysics in 3d transition metal complexes, but have also application in the understanding of optical writing/magnetic reading in spin crossover (SCO) compounds.[7] Moreover such complexes were thought as potential substitutes for Grätzel-type dye-sensitized photovoltaic cells.[8] Indeed these diamagnetic low-spin d⁶ diimine complexes are considered as models for Fe(II) SCO complexes which quite commonly present N₆ coordination spheres based on heteroaromatic ligands. Comparatively, SCO complexes usually show much smaller zero-point energy difference ΔH_{HL} (≈1000 cm⁻¹) between the high-spin (HS) configuration, for low ligand-field (LF) strength, and the low-spin (LS) configuration, for high LF strength.[9,10] It is known for SCO complexes that in the solid state the low temperature LS ground state may be photoconverted to a long-lived metastable HS state, the so-called Light-Induced Excited Spin State Trapping (LIESST) effect.[11,12] It was shown even earlier that such photoconversion could take place in solution at about room temperature using pulsed irradiation with corresponding fast relaxations.[13] Fe(II) LS polyimine complexes, while having much higher ΔH_{HL} (≈6000 cm⁻¹), show nevertheless

the same conversion to a metastable HS state by ultrafast optical pumping, with even faster corresponding relaxations.[1,4,6,14–25] While these compounds exhibit many interesting features for optical applications, their use in optics is still limited due to the centrosymmetry that most of Fe(II) complexes with polyimine ligands usually adopt in solid state. This centrosymmetry prevents these compounds from exhibiting interesting properties such as piezoelectric and electro-optic effects, as well as second order non-linear optical phenomena giving rise to second harmonic and sum frequency generation. To further extend the application of Fe(II) complexes, it is necessary to break their natural centrosymmetry.

One strong point of molecular materials is the endless chemical playground they represent for grafting new properties. Notably, we have been investigating the combination of SCO and chirality for some years now,[26] a combination sometimes obtained by serendipity[27] and obtained rationally only using optically active ligands.[27–34] Due to their extensively studied photophysics, the model complexes [Fe(*bipy*)₃]²⁺, [Fe(*phen*)₃]²⁺, or [Fe(*terpy*)₂]²⁺ were evident targets for attractive low-cost non-centrosymmetric materials showing non-linear optical properties, and for the study of their eventual dependence with the spin state of the complex. Indeed some data were recently published on a SCO compound, but puzzlingly the reported crystalline structure is centrosymmetric, and the magnitude of the effect reported was quite weak.[35] In view of those

results, we decided to pursue the study of the chiral induction of the model complex [Fe(*phen*)₃]²⁺ by a series of chiral anions.

We used two families of chiral anions (Figure 1): D_2-symmetric anions based on cheap and easily available tartaric acid such as arsenyl/stibyl tartrate adducts, and D_3-symmetric anions, tris(catechol)phosphate(V) (TRISCAT), tris(catechol)arsenate(V) (TRISCAS) and 3,4,5,6-tetrachlorocatechol phosphate(V) (TRISPHAT). TRISCAT is easily accessible, but it epimerizes quickly in solution and loses its optical activity.[36] However, TRISCAS was reported to be stable in solution and was resolved to Δ and Λ isomers using cinchonine and cinchonidine alkaloids respectively.[37,38] Likewise, TRISPHAT was resolved with high diastereomeric excess using chiral alkaloids,[39,40] and has been used in asymmetric chemistry as resolving agent for high levels of induction or recognition in molecular[41,42] or supramolecular processes.[43] Surprisingly, they have been used so far only sparsely for the synthesis of materials.[44] There are only few reports of diastereoselective ion pairing of the TRISPHAT anion with diimine low-spin Fe(II) complexes, either in solution,[41,42,45,46] or in the solid state.[43,47,48]
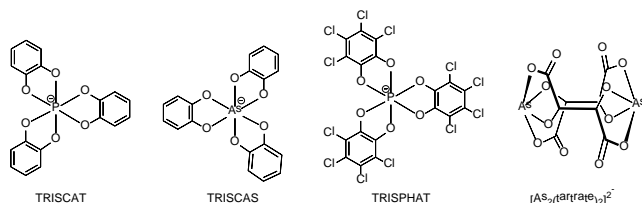

Figure 1. Schematic representation of D_3-symmetric chiral anions (TRISCAT, TRISCAS, TRISPHAT) and D_2-symmetric chiral arsenyl tartrate anion.

On the other hand, the D_2-symmetric As(III)[49] or Sb(III)[50] tartrate adducts were used in the past for the resolution of metal complexes,[45,51–55] mainly through chiral HPLC,[53,56–58] with C_2 and C_3 association models proposed for the chiral recognition of octahedral metal complexes by [Sb₂(tartrate)₂]²⁻.[59,60] Their synthesis is based on easily available and cheap tartaric acid. Potassium (+)-antimonyl tartrate is even commercially available, but its insolubility in organic solvents limits severely its usefulness. The chirality of these anions can be simply labelled by extending the IUPAC skew line system (Scheme 1),[61] with one line joining the carboxylate coordinated oxygen atoms of one tartrate ligand and the second line the twofold axis intersecting the As atoms.[#] This is indeed similar to the accepted convention for tris(bidentate) octahedral complexes,[62] when considering one ligand and the threefold axis of the complex (Scheme 1).[61]

Chiral [Fe(*phen*)₃]²⁺ complexes show strong non-linear optical properties as shown in our recently published study on second-harmonic generation, its correlation with the electronic absorption spectrum, and sum-frequency generation for drop-cast films of the complex resolved with the arsenyl tartrate anion that is published elsewhere.[63] Herein we present a full report on the synthesis and characterization in solution and in the solid state of such materials resolved with two families of anions (see table of compounds in Supplementary Information). Dichroic optical studies allowed us to compare the chiral induction in the solid state and in solution. While optically pure complexes with TRISPHAT could not be isolated, complexes containing the TRISCAT and TRISCAS anions were shown to crystallize as inversion twins in the Sohncke $R32$ space group, the Flack/batch parameter being close to the optical purity of the starting anion. The arsenyl tartrate anions yielded instead structures in the enantiomorphic $P3_121/P3_221$ space groups. Those molecular materials, soluble in some common organic solvents, can be easily drop-cast as films. Non-linear optical studies on drop-cast films of the complex resolved with the TRISCAS anion revealed very strong second-harmonic generation. The intensity of the signal monitored in function of the excitation wavelength showed a strong correlation with the electronic spectrum and its dichroic counterpart. This work opens the way to novel studies at room temperature on non-linear optical properties dependence upon modulation of the spin state[64] by ultrafast pumping.
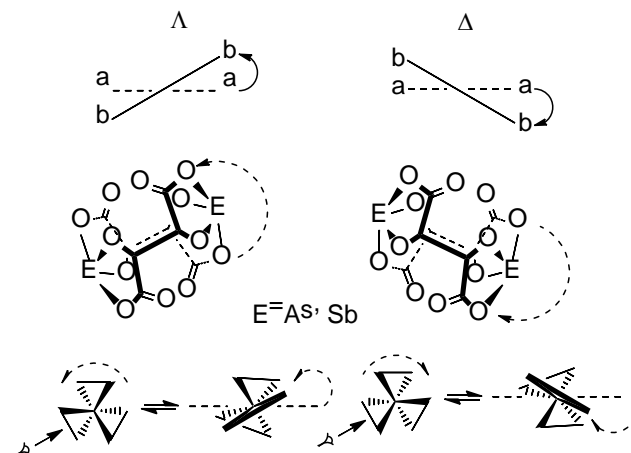

Scheme 1. Definitions of the Δ and Λ configurations in arsenyl/stibyl tartrate anions and octahedral complexes.

Results and discussion

Synthesis and characterization of chiral anions.

Syntheses of TRISCAT, TRISCAS and TRISPHAT were reproduced or adapted from previous literature and are reported in Supplementary Information. While synthesis of the arsenyl tartrate adducts readily yields Δ-**1**, Λ-**1**, or *rac*-**1** as confirmed by elemental analysis (Scheme 2), instead reactions with antimony trioxide did not give satisfactory analyses. In agreement with previously published structures for other derivatives of this dianion,[49,50] they demonstrate D_2 symmetry: (−)-(S,S)-tartaric acid gives the Δ isomer while the adduct with (+)-(R,R)-tartaric acid is the Λ isomer,[#] as shown by crystal structures solved in the Sohncke[&] $P2_12_12$ space group (see details in Table SI2 and Figure SI3 in Supporting Information). Polarimetry and FTIR show that anion **1** in solution is likely to partially decoordinate, but regains the D_2 structure upon solvent removal (see details in Supporting Information). Accordingly, a further study of the arsenic and antimonyl tartrate anions in solution by vibrational dichroic studies will be reported elsewhere.
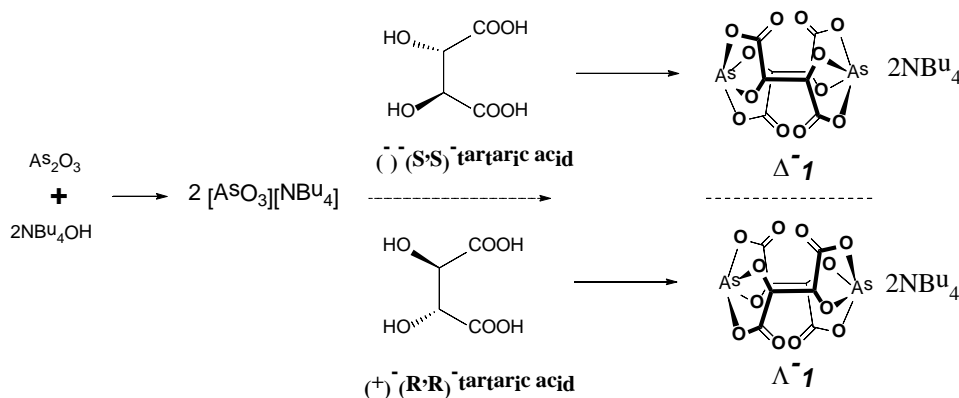
Scheme 2. Synthetic path to chiral anion **1**.

[Fe(phen)₃](X)₂ (X = TRISCAT (2); TRISCAS : rac (3), Δ (4), Λ (5))

No Fe(II) complexes based on TRISCAT or TRISCAS have been reported in literature before, the only examples with TRISCAS being Cu(II) complexes.[65,66] The synthetic procedure consisted in all cases in layering a methanolic iron sulphate solution over solutions of TRISCAT.HNBu₃ or TRISCAS racemic/Δ/Λ salts and 1,10-phenanthroline (*phen*) in a mixture of methanol and dichloromethane. Red single crystals were formed in a few weeks. Diffraction data for [Fe(*phen*)₃](*rac*-TRISCAT)₂ (**2**), [Fe(*phen*)₃](X-TRISCAS)₂ (X = *rac* (**3**), Δ (**4**), Λ (**5**)) were collected. As shown by almost identical cell parameters between complexes **2-5,** they are isomorphous. The data could be satisfactorily integrated in the trigonal system, but scaling and merging could be performed either in the -3 or -3*m* Laue class.

In order to select the correct space group within the corresponding point groups (-3m, 3m, 32, -3 and 3) belonging to those two Laue classes, a dataset collected on complex **4** integrated in trigonal settings but scaled and merged in point group *P*1 was further analyzed (see details and Table SI6 in Supplementary Information).[67]

The intensity data were then sorted into sets of 12 reflections symmetry-equivalent under point group -3*m*, of which 45 complete sets were obtained. We calculated then for each point group R_{merge} for $|F_{obs}|^2$, A and D (A and D being the average and the difference of Friedel opposites respectively).[68–74] There was a clear preference for non-centrosymmetric point groups 3 and 32. Systematic extinctions led to potential *R*3 and *R*32 space groups respectively. The structures could be solved in either space group. Full convergence required the inclusion of an inversion twin law for all complexes **2-5**, and final refinement statistics were systematically slightly better for the *R*32 space group. The X-ray crystallographic refinement data for complexes **2-5** are shown in Table SI9 in Supporting Information. Flack parameters were obtained after full convergence of the structures: for complexes **2-5**, it deviates significantly from zero at 0.45(2), 0.473(15), 0.163(13) and 0.277(2) respectively. Those values were apparently close to the optical purity of the starting anion: TRISCAS diastereomeric excesses were 0% for **2**-**3**, 88% for **4**, while it was 66% for **5**. Nevertheless, when we performed a second synthesis of complex **4** with an 86% d.e. batch of Δ-TRISCAS, the resulting crystal analyzed yielded a Flack parameter statistically equal to zero (complex **4a** at -0.006(3)), evidencing that the link between crystals and starting anion optical purity is not completely straightforward.

The fact that complexes **2**-**3** did not crystallize in a centrosymmetric space group as expected led us to check the veracity of the existence of these inversion twins. Indeed, it has been found true that most non-centrosymmetric crystal structures with Flack parameter values between 0.25 and 0.75 published in *Acta Cryst. C* in 2011 and 2012 were in fact twinned by inversion.[75–77] We thus analysed the data further, with refinement completed without the twin law for complexes **3** and **4** (see more details and Figures SI7 and SI8 in Supporting Information). Observed and modelled data were then separated in centric and acentric reflexions. [68–77] The slopes given by the plots of Dobs (difference for paired observed Friedel reflections) vs. Dsingle (difference for paired Friedel reflections calculated from a single domain model) were in perfect agreement with the Flack parameter issued from the least-square refinement including the racemic twin law, evidencing that those compounds are indeed racemic twins. One must note that crystals observed under polarized light did not evidence macroscopic domains of opposite handedness. The inversion twin implies then the presence of microscopic domains of opposite handedness that are intimately mixed.

The global description of all crystal structures is similar. As expected, the interaction of the bulky TRISCAT or TRISCAS counter ions with the [Fe(*phen*)₃]²⁺ system does not modify the spin state of the tris-phenanthroline iron(II) system. The average iron-nitrogen bond distance is Fe-N$_{avg}$ ≈ 1.97 Å, corresponding to the LS state due to the strong σ-donating and π-back bonding capabilities of the ligand molecule.[78] The [Fe(*phen*)₃]²⁺ complex and two TRISCAT/TRISCAS anions form triads by interacting strongly along the complex 3-fold axis (Figure 2), the distances between iron and anion being d$_{Fe-P}$ = 5.6889(8) Å and d$_{Fe-As}$ = 5.7162(16) Å for complexes **2** and **3** respectively.
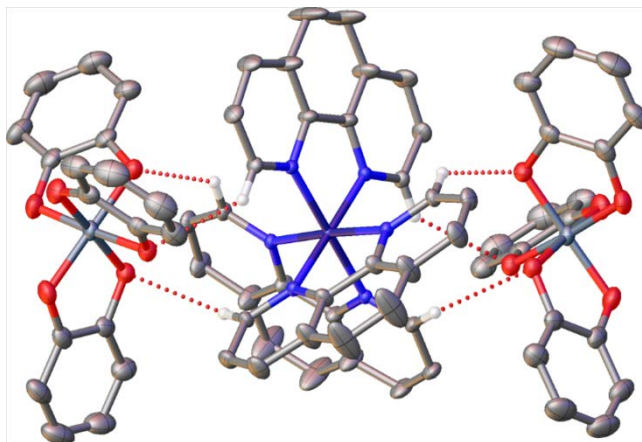
Figure 2. Axial interactions of two Δ-TRISCAS with the 1,10-phenanthroline α acidic hydrogens of a [Λ-Fe(*phen*)₃] complex in complex [Fe(*phen*)₃](rac-TRISCAS)₂ (**3**).
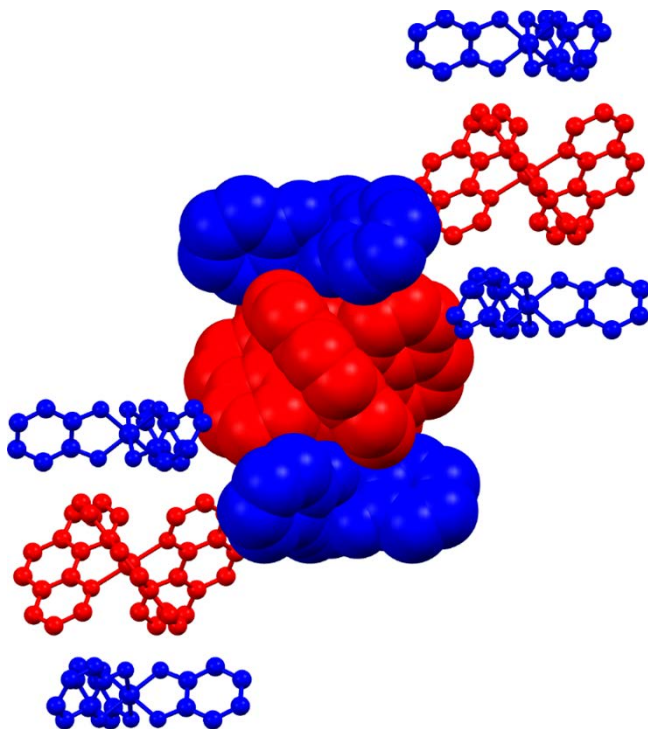
3

Figure 3. Staggered interactions between a given triad (van der Waals representation, Δ TRISCAS in blue and Λ Fe(II) in red) and two triads of its shell, as seen perpendicularly to the *c* axis.

Each complex is surrounded by six anions, forming a shell along the crystallographic *c* axis (see more details in Supporting Information, Figure SI11), with each anion of this shell itself part of another triad. Those triads are staggered alternatively above and below (Figure 3). The dichloromethane molecules fill the void spaces between the triads. The average contacts and distances between cations and anions for complexes **2**-**5** are very similar (Supporting Information, Table SI10). We observe heterochiral interactions within the triads, mediated mainly through hydrogen bonding between the α-acidic hydrogens of the phenanthroline ligand and the oxygen atoms of the anion (C-H•••O ≈ 3.3 Å) and some aromatic carbons (C-H•••$C_{(\pi)}$ ≈ 3.5-3.7 Å), completed by a strong oxygen-carbon π-π interaction ($O_{(\pi)}$•••$C_{(\pi)}$ ≈ 3.1-3.2 Å). X-ray powder diffractograms for complexes **3**-**5** confirmed that the crystalline phases we evidenced are the only ones present: experimental and calculated diffraction patterns from the corresponding X-ray structures agree perfectly (Supporting Information, Figure SI12).

While trying to obtain drop-cast films for the NLO measurements described below, solutions of twinned crystals of **3** and **4** in acetonitrile yielded isostructural solvatomorphs, as acetonitrile solvated crystal structures (**4b**-**5b** and **4c**-**5c**, Table SI13 in Supporting Information). Spontaneous resolution occurs, yielding conglomerates of enantiopure crystals. This is in contrast with the recently reported copper complexes resolved using the TRISCAS anion which evidenced enhanced racemization of the anion in a mixture of dichloromethane and acetonitrile.[65] Nevertheless, *R*32 being an achiral Sohncke space group, crystals of opposite handedness show achiral morphologies and cannot be sorted mechanically.
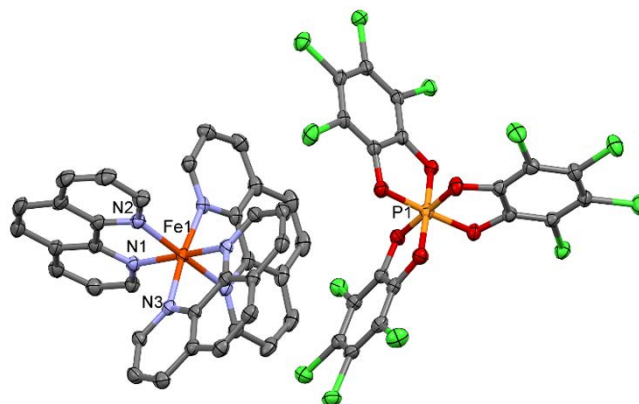

Figure 4. Complex [Fe(*phen*)₃](*rac*-TRISPHAT)₂ (**6**) measured at 120 K. H atoms have been omitted for clarity, with displacement ellipsoids drawn at the 50% probability level.

[Fe(phen)₃](rac-TRISPHAT)₂ (6)

As we mentioned, there have been a few reports studying the chiral induction of the TRISPHAT anion on some diimine Fe(II) complexes, but those were limited to solution studies (NMR and CD measurements).[41,42,45,46] In order to obtain structural data, we obtained crystals in a few days by layering a methanol solution of iron(II) sulphate over a solution of the *phen* ligand and the corresponding salt of TRISPHAT anion. When using *rac*-TRISPHAT, we observed two distinct crystals morphologies: on one hand hard deep-red well-defined prisms, and on the other hand crumbly red-orange flat crystals. With enantiopure Δ-TRISPHAT, only the flat orange crystals were obtained, while a Λ-TRISPHAT batch with a low d.e. excess, and thus containing a significant amount of the racemate, yielded again a mixture of phases. Despite many trials, only the hard-red prisms allowed us to solve and refine the corresponding structure in the centrosymmetric monoclinic *C*2/*c* space group. The reaction with Δ-TRISPHAT would have suggested that the red-orange phase may be the looked-for non-centrosymmetric one, and that some spontaneous resolution may occur even with the racemic anion. Unfortunately this phase is very fragile and likely to be very heavily solvated, and crystals do not survive either manipulation or being outside the mother liquor. Dichroic spectra measured in a 99:1 CHCl₃/DMSO mixture did not show any signal, though this solvent mixture was reported to yield a d.e.>95% for TRISPHAT.[41,42] The centrosymmetric structure corresponds to the expected Fe(II) complex (see Figure 4 and Table SI14 in Supporting Information for further details), with half of it and a TRISPHAT anion making up the asymmetric unit. This phase is also heavily solvated, with huge solvent-accessible spaces accounting for almost 1/3 of the unit cell volume, and the SQUEEZE procedure[79] had to be applied to allow a satisfactory refinement, yielding [Fe(*phen*)₃](*rac*-TRISPHAT)₂.(CH₂Cl₂)ₙ (**6**) (4 ≤ n ≤ 16).

The low-spin Fe(II) complex has an average Fe-N bond length of 1.982(1)Å. When looking at the crystal packing, with the provision that interactions with the solvent molecules cannot be analyzed due to disorder, no particularly relevant interaction between iron complex and phosphate anions can be observed. Overall those results are really surprising considering previous solution NMR and CD studies which stated that "diastereoselective induction from TRISPHAT anions onto tris(diimine)iron(II) complexes occurs with better selectivity with *phen* rather than *bipy* ligands".[41,42]

[Fe(phen)₃](X) (X = As₂(tartrate)₂ : Δ (7), Λ(8), racemic mixture (9)

A solution of the corresponding $(NBu_4)_2[\Delta/\Lambda\text{-}As_2(\text{tartrate})_2]$ anion **1** was layered with a solution of $[Fe(phen)_3]^{2+}$ to form crystals of complexes $[Fe(phen)_3](X)$, $X= \Delta\text{-}As_2(\text{tartrate})_2$ (**7**) and $\Lambda\text{-}$ (**8**). The crystal structures could be solved and refined to convergence in the enantiomorphic $P3_121/P3_221$ space groups respectively. Crystallographic data are reported in Table SI15 in Supporting Information. Unit cells of **7** and **8** are very similar to the analogous complex of $[Fe(phen)_3]^{2+}$ with $[\Lambda\text{-}Sb_2(\text{tartrate})_2]^{2-}$ that crystallizes in the same trigonal chiral space group $P3_221$.[52] These phases showed again to be heavily solvated, with huge solvent-accessible spaces accounting for almost 1/3 of the unit cell volume. No satisfactory discrete disorder model was achievable, so the SQUEEZE procedure had also to be applied to allow a satisfactory refinement, yielding a likely composition $[Fe(phen)_3][As_2(\text{tartrate})_2](MeOH)(CH_2Cl_2)_4$. Crystal structures of **7** and **8** are enantiomorphous with the same unit cell, each asymmetric unit consists of half a cation and half an anion (Figure 5) lying over crystallographic twofold axes. The cation molecular symmetry is nevertheless very nearly threefold. The iron atom is clearly low-spin in both case with an average Fe-N bond length of 1.968(3) Å and 1.970(6) Å for **7** and **8** respectively. Flack parameters for **7** and **8** are statistically different from zero but quite close to it, showing that the crystals are almost enantiopure. Synthesis with an equimolar racemic mixture of $(NBu_4)_2[\Delta/\Lambda\text{-}As_2(\text{tartrate})_2]$ yielded similar looking crystals of complex **9** (Figure 5). The crystal structure could be solved and refined as a racemic twin in the $P3_121$ space group, with a batch factor of 0.492(13), as already observed for $[Fe(phen)_3](rac\text{-}TRISCAS)_2$ (**3**).

Cation and anion interact homochirally in complexes **7** and **8** (Figure SI16 in Supporting Information): the helicity of $[Fe(phen)_3]^{2+}$ is induced by the configuration of the D_2 arsenyl tartrate. This is again similar to the previously reported structure with antimonyl tartrate.[52]

The crystal packing is identical for **7-9**. The cations form layers between which $[As_2(\text{tartrate})_2]^{2-}$ anions are embedded in order to compensate the charge of the layers (Figure SI17 in Supporting Information). Six anions are interacting with each $[Fe(phen)_3]^{2+}$ and have the same configuration as the cationic complex. Four of them are almost equidistant ($d_{Fe\text{-}As} \approx 6.1$ Å) and two are farther away ($d_{Fe\text{-}As} \approx 9.5$ Å). This is opposite to the isostructural $[\Lambda\text{-}Fe(phen)_3](\Lambda\text{-}Sb_2(\text{tartrate})_2)$ complex where the Fe-Sb distances of the four nearest anions are unequal (5.884 Å and 6.233 Å) and other two anions are at longer distances (9.80 Å).[52]

The four closest anions are interacting with the cationic complex along two of the twofold and threefold symmetry axes of the complex (Figure 6). The homochiral interaction is mediated through hydrogen bonds between the oxygen atoms of the tartrate and hydrogen atoms of the aromatic rings of the complex ($O_{\text{anion}}\bullet\bullet\bullet C\text{-}H_{\text{complex}} \approx 3.146(4)$ Å, 3.337(3) Å). Theses distances are similar to those found for antimonyl tartrate ($O_{\text{anion}}\bullet\bullet\bullet C\text{-}H_{\text{complex}} \approx 3.198(4)$ Å, 3.317(3) Å).

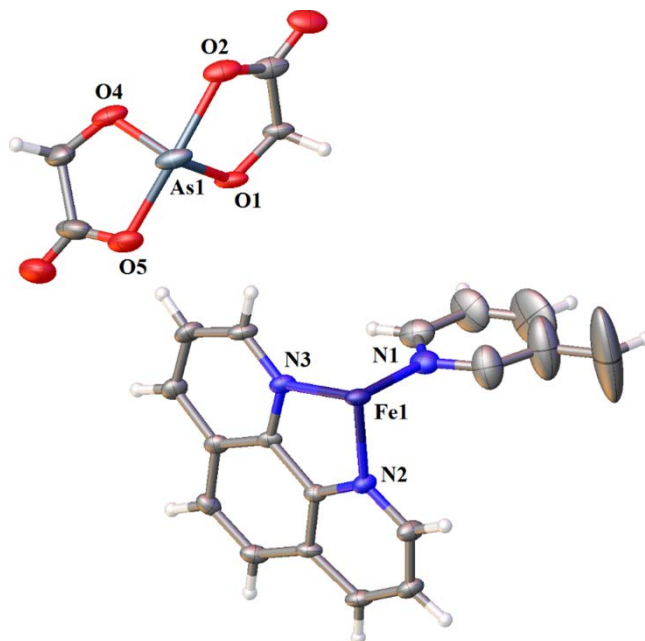Figure 5. Asymmetric unit of complex $[Fe(phen)_3](As_2(\text{tartrate})_2)$ (**9**) at 120K. Displacement ellipsoids are drawn at the 50% probability level.
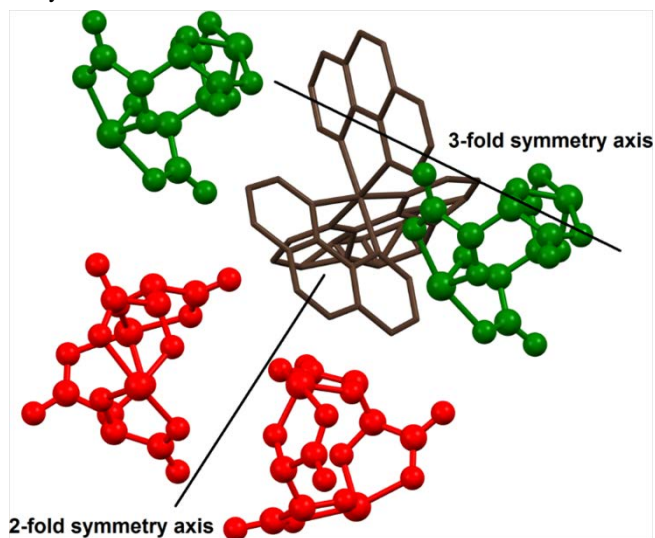
Figure 6. Interaction of the four closest $[\Delta\text{-}As_2(\text{tartrate})_2]^{2-}$ anions with $[\Delta\text{-}Fe(phen)_3]^{2+}$ along 3- and 2-fold symmetry axes of complex **7**.

Powder X-ray diffractograms measured for complexes **7-9** show an excellent match between experimental and calculated patterns from the single crystal structures (Supporting Information, Figure SI18), confirming the presence of one single phase in the bulk product.

Electronic absorption and circular dichroism of complexes 2-5 and 7-9

The tris-chelation of a metal by conjugated aromatic ligands is well understood, leading to exciton splitting[80] of the three degenerate ligand $\pi - \pi^*$ transitions in the UV region in a so-called CD couplet with opposite rotatory strengths, with a pattern correlated with the helicity of the ligands disposition.[81] Indeed the intensity of the two dichroic bands is induced by the helical disposition of the $\pi - \pi^*$ transitions and the resulting charge displacement by coulombic

coupling. Reference spectra are available for TRISCAS (water solution):[82,83] two π-π* catechol transitions were observed in water solution at 220 and 276 nm, but only the high-energy transition has dipole moments oriented in such a way to interact and give a couplet. Only the couplet low energy component could be measured at 226 nm with positive Cotton effect ($\Delta\varepsilon = +68$ Lmol^{-1}cm^{-1}) for the Λ configuration.[82,83]

We measured CD spectra for both anion **1** and the easily accessible K$_2$[Sb$_2$(tartrate)$_2$] (Figure SI19 to SI21 in Supporting Information), as compared to published spectra of tartrate. Dianionic tartrates show bands at 194 and 211 nm assigned to n-π* and n-σ* forbidden transitions of the carboxylate groups, with no excitonic coupling seen outside supramolecular packings.[84–86] The CD spectra in water for K$_2$[Sb$_2$(tartrate)$_2$] and MeCN for anion **1** show instead two excitonic couplets: one at lower energies, centered at 223 nm for K$_2$[Sb$_2$(tartrate)$_2$] and at 219 nm for anion **1**; the second one at 200 and 197 nm respectively. In both cases, excitonic couplets are of positive (respectively negative) chirality for the Λ (respectively Δ) anion configuration, which upon inspection of the crystal structures do not correspond to the coupling of the transitions observed for dianionic tartrate. This combined with the observed bathochromic shift supports that electronic transitions are different for As and Sb tartrate adducts, with the deprotonated hydroxyles of the tetraanionic tartrates likely to play a role. Anion **1** is sparingly soluble in water, and the corresponding spectra are seen to be strikingly similar to those of (NBu$_4$)$_2$(tartrate), supporting that according to the solvent partial or total decoordination of the tartrate may occur. Further dichroic studies in solution will be reported elsewhere. In the solid state (Figure SI22 in Supporting Information), KBr pellets of Δ-**1** and Λ-**1** show what could be part of excitonic couplets below 230 nm. The difference in the Cotton effect between Δ-**1** and Λ-**1** is likely due to inevitable experimental errors in preparing the KBr pellets. To the best of our knowledge no further CD spectra were previously reported for tartrate adducts with As(III) or Sb(III).

Reference spectra are available for [Fe(*phen*)$_3$]$^{2+}$ in water solution: one π-π* *phen* transition was observed to give a couplet at 260 nm and 272 nm, which are A$_2$ and E coupled in the D_3 symmetry point group.[87] The two bands show opposite Cotton effect, negative at 272 nm for the Δ configuration and inversely positive for the Λ configuration ($\Delta\varepsilon = +715$ Lmol^{-1}cm^{-1}), confirmed from the crystallographic structure of [Λ-Fe(*phen*)$_3$]$^{2+}$.[52]

Electronic spectra for complexes **2-5** and **7-9** in acetonitrile solutions are shown in Figure 7 and 8, with further details in Figure SI23 to Table SI26 in Supporting Information. The TRISPHAT asymmetric induction towards [Fe(phen)$_3$]$^{2+}$ in solution has been extensively studied by circular dichroism and 1H-NMR,[41,42] so we studied the effectiveness of optically active TRISCAS towards the same cation. Efficient asymmetric induction was evidenced towards robust dinuclear helicate copper(II) species, but it was pointed out that asymmetric induction was affected by the possible protonation of the anion and the donating character of the solvent.[65,66]
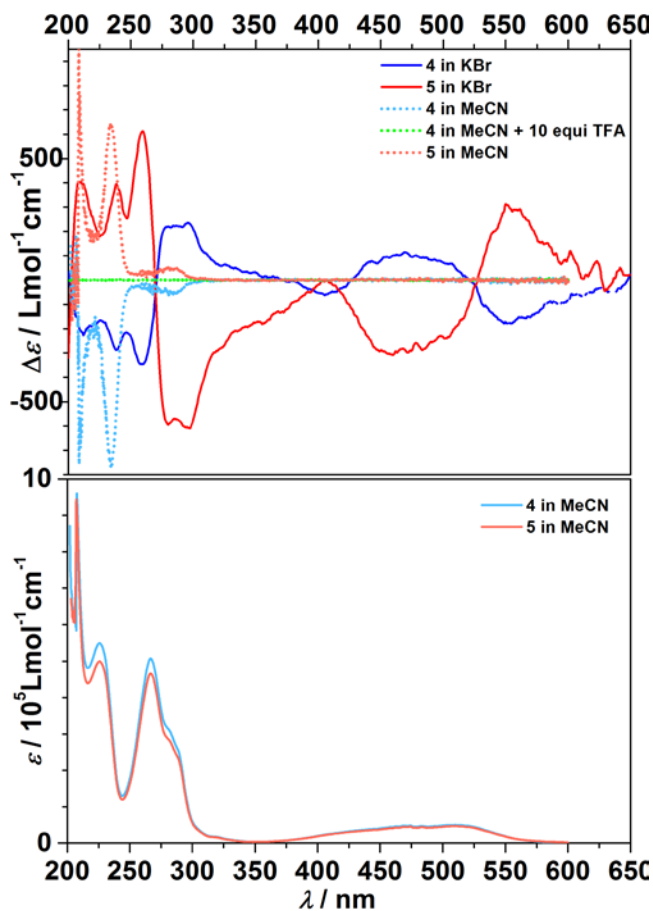

Figure 7. (top) CD spectra : **4** (blue shades) and **5** (red shades) in KBr pellets (full lines) and in acetonitrile solution (short dotted line), and **4** in acetonitrile solution + 10 eq TFA (short dotted green line); (bottom) corresponding UV-visible spectra of **4** and **5** in acetonitrile solution.

The [FeN$_6$]$^{2+}$ core is known for its lability.[51] Nevertheless we measured the CD spectra in acetonitrile for complexes **4** and **5** (Figure 7, top) and complexes **7** and **8** (Figure 8, top). It is clear from Figure 7 and 8 that in acetonitrile solution no [Fe(*phen*)$_3$]$^{2+}$ MLCT bands are present. [Fe(*phen*)$_3$](TRISCAS)$_2$ (Figure 7) shows only three Cotton effects at 209 nm, 234 nm and 280 nm ($\Delta\varepsilon$ of +1004, +643 and +50 Lmol^{-1}cm^{-1} respectively for **4**), inverted for **5** ($\Delta\varepsilon$ of -758, -755 and -48 Lmol^{-1}cm^{-1} respectively). Those features correspond only approximately to the TRISCAS catechol $\pi - \pi^*$ transitions reported previously.[81] Indeed the couplet reported at 220 nm is not apparent here, and transitions appear to be much more intense. Nevertheless Λ/Δ-TRISCAS alkaloid salts when measured in acetonitrile instead of water were seen to show transitions with pronounced hypsochromic shifts and enhanced intensities (Figure SI27 in Supporting Information). The low-energy band of the couplet is shifted to 206 nm, the uncoupled transition to 235 nm, and a further transition is seen at 280 nm, with $\Delta\varepsilon$ = -96, -46 and -3 Lmol^{-1}cm^{-1}, +151, +73 and +5 Lmol^{-1}cm^{-1} for cinchoninium(Δ-TRISCAS) and cinchonidinium(Λ-TRISCAS), respectively. The absence of any Cotton effect corresponding to the MLCT bands in the visible region and the similarity with the anion CD spectra indicates for the complex that dissociation of the ion pair occurs with subsequent racemization of the Δ− or [Λ-Fe(*phen*)$_3$]$^{2+}$ complexes through the well-known Bailar or Rây-Dutt twist mechanisms.[88] The link of these UV features with

TRISCAS is confirmed by the complete loss of optical activity for the [Fe(*phen*)₃](Δ-TRISCAS)₂ solution (Figure 7) upon addition of a few drops of trifluoroacetic acid: the acidic racemization of Δ-TRISCAS is well documented.[89] For [Fe(*phen*)₃](As₂(tartrate)₂), the CD spectra for **7** and **8** (Figure 8) are clearly very similar to the ones we recorded for anion **1** in MeCN (Figure SI20 in Supporting Information). The ion-pair dissociation and subsequent quick racemization observed here is puzzling since antimonyl(tartrate) was used to prepare optically pure [Fe(*phen*)₃]$^{2+}$ samples on which dichroic spectra were originally measured in much more polar water.[87]
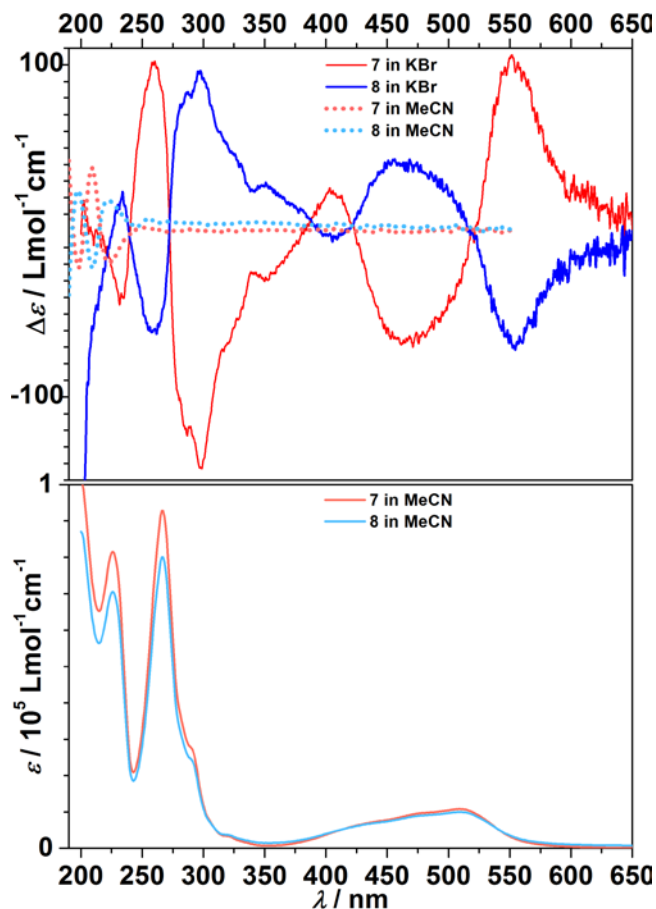

Figure 8. (top) CD spectra : **7** (red shades) and **8** (blue shades) in KBr pellets (full lines) and in acetonitrile solution (short dotted line); (bottom) corresponding UV-visible spectra of **7** and **8** in acetonitrile solution.

We also checked whether any chiral induction could be seen in solution by recording ^{1}H NMR spectra for complexes **3** and **4** in CD₃CN and (CD₃)₂CO (Figures SI28 in Supporting Information). In both cases spectra are seen to differ for hydrogen atoms in *ortho* and *para* positions from the spectrum recorded for [Fe(*phen*)₃]Cl₂ in CD₃CN,[90] suggesting close ion pairing in solution. Nevertheless, the absence of [Fe(*phen*)₃]$^{2+}$ MLCT bands in the CD measurement in both acetonitrile and acetone would indicate that this interaction is not close enough to prevent racemisation of [Fe(*phen*)₃]$^{2+}$. The low solubility of complex **4** in non-polar solvents prevented studying the effect of the polarity of the solvent.

As shown by the crystal structure, there is clearly an efficient asymmetric induction in the solid state. While measurement of dichroic spectra in the solid state is usually very tricky, due to macroscopic anisotropies such as linear dichroism and birefringence, which may be of similar or greater amplitude than the CD signal, and which may couple with non-ideal characteristics of the polarization modulation,[91] dispersion of microcrystalline powder in KBr pellets solves partially this issue.[92] We measured CD spectra of KBr pellets with complexes **4** and **5** (7.2 mmol/dm³, thickness = 0.35 mm) at room temperature (Figure 7). The [Fe(*phen*)₃]$^{2+}$ MLCT bands are observed this time, as alternating bands at 555, 470 and 405 nm (Δε of -178, +114 and -61 Lmol⁻¹cm⁻¹ respectively for **4**, and mirroring intensities of +284, -291 and -0.5 Lmol⁻¹cm⁻¹ for **5**).

The intense π–π* absorption bands in the UV-region (200–400 nm) correspond to electronic transitions of TRISCAS and 1,10-phenanthroline that are overlapping. Nevertheless, couplets for both chromophores can be observed. Indeed, for complex **4** the couplet corresponding to the high-energy π–π* phen transitions is observed at 280 and 260 nm (Δε +220 and -346 Lmol⁻¹cm⁻¹ respectively), its sign corroborating the Λ configuration observed in the X-ray structure. Surprisingly, the low-energy transition gives significant dichroic signal at 296 nm (Δε +236 Lmol⁻¹cm⁻¹). The Δ-TRISCAS catechol couplet high-energy component is observed at 212 nm (Δε -226 Lmol⁻¹cm⁻¹), with the uncoupled transition at higher wavelength at 238 nm (Δε -287 Lmol⁻¹cm⁻¹). The Λ-TRISCAS complex **5** shows correspondingly opposite Δε values: -595 and +611 (phen couplet), +608 (296 nm), +395 (catechol couplet) and +391 Lmol⁻¹cm⁻¹ (238 nm). When recrystallizing the complex in acetonitrile, the CD spectrum of a KBr pellet prepared from a single crystal showed very similar CD spectra to the parent compound (Figure SI29 in Supporting Information). Δε values for the single crystal pellet are puzzlingly very close to the ones obtained from the starting complex prior to recrystallization, which supposedly was less optically pure.

Mirror images CD spectra for KBr pellets of **7** and **8** are shown on Figure 8. The [Fe(*phen*)₃]$^{2+}$ MLCT bands are again observed at approximately 555, 470 and 405 nm (Δε of +97, -67 and +24 Lmol⁻¹cm⁻¹ respectively for **7**, -70, +40 and -6 Lmol⁻¹cm⁻¹ respectively for **8**). In the UV range, five Cotton effects are seen at 350, 298, 285, 260 and 233 nm (Δε -30, -142, -119, +102 and -38 Lmol⁻¹cm⁻¹ respectively for **7**, +27, +96, +81, -59 and +19 Lmol⁻¹cm⁻¹ respectively for **8**). The 285 and 260 nm are the high-energy *phen* couplet and its sign correspond to the crystallographic Δ- and [Λ-Fe(*phen*)₃]$^{2+}$ for complexes **7** and **8** respectively. The lower energy transition at 298 nm was already observed in complexes **4** and **5**, but the well-defined feature at 350 nm was not present and remains unexplained. The higher Cotton effect at 233 nm may be linked to the [As₂(tartrate)₂] dianion.

Second-harmonic generation experiments

As discussed above, one of the main interests in the use of chiral anions is that they will ensure that a given material will crystallize in a non-centrosymmetric space group that may exhibit second-order nonlinear optical properties. We checked that indeed the chiral complexes we synthesized exhibit such properties by performing second harmonic generation (SHG) experiments. The principle of these experiments is very simple: exciting the sample with intense laser pulses, the second-harmonic signal (SHS) is recorded at the exit of sample or in reflection at its surface. In short, the experimental set-up we used is as follow. Laser pulses provided at 60 kHz repetition rate by an optically parametric amplifier were focused on the sample by mean of a 20 cm focal length lens. The energy of 160 fsec pulses, tunable in the 2.4 μm -0.6 μm spectral range, can be as high as 60 μJ. The SHS generated is collected in transmission at the exit of the sample and it is focused at the entrance slit of a spectrometer connected to a CCD camera. To reject the light at the

fundamental laser frequency a filter was inserted in front of the spectrometer.

Samples were prepared by drop casting a small volume of solutions of complexes **4** and **5** (see Supplementary Information for further details). We found that acetonitrile solutions resulted in the formation of rather large microcrystallites. Instead with N,N-dimethylformamide we observed rather good quality films on the dried samples, with small crystallites no larger than a few micrometers in size randomly dispersed (see Figure SI30-31 in Supporting Information). Preservation of the molecular structure was evidenced by Raman spectroscopy on those films as compared with bulk single-crystals, and conservation of the structure was checked by X-ray diffraction (see Figure SI32 in Supporting Information).
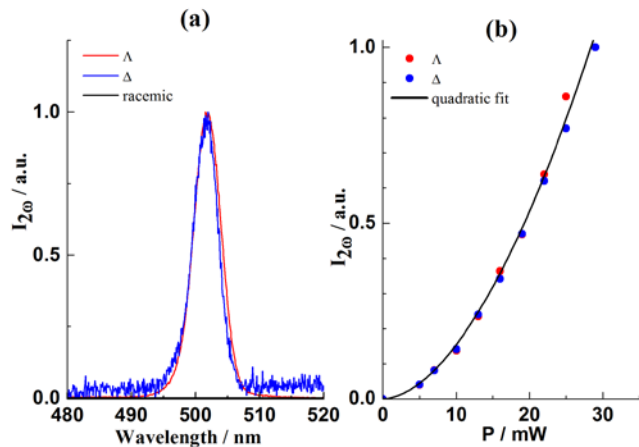

Figure 9. a) Spectra of the SHS recorded for the two enantiomers (**4** and **5**) and the racemic mixture (**3**) excited by femtosecond pulses centered at λ=1050 nm. b) Evolution of the SHS intensity versus the intensity of the fundamental pulse. The blue and red dots are the experimental data for the two enantiomers, the straight line is a fit considering a quadratic dependence.

The spectra of the normalized SHS we recorded for films prepared from [Fe(*phen*)$_3$](Δ-TRISCAS)$_2$ (**4**) and [Fe(*phen*)$_3$](Λ-TRISCAS)$_2$ (**5**) when the excitation wavelength is fixed at λ = 1004 nm are displayed in Figure 9. These spectra are centred at $\lambda/2$ = 502 nm (Figure 9a). Moreover, as expected for a non phase-matched optical second-order nonlinear phenomena, the amplitude SHS in both samples evolves as the square of the fundamental pulse intensity (Figure 9b). This ensemble of results clearly indicates that the recorded signal results indeed from SHG. We have performed the same experiment on a drop-cast of a racemic solution of [Fe(*phen*)$_3$](TRISCAS)$_2$ (**3**). Under the same experimental conditions, we could not detect any SHG signal. This experiment confirms that the racemic sample is not optically active and therefore does not exhibit any second order nonlinear optical properties.

Finally, we also measured the evolution of the SHS when we tuned the central wavelength of the excitation pulses. The SHS we recorded at λ = 1050 nm is displayed against the signal we recorded at λ = 1350 nm and λ = 800 nm (Figure 10). These three signals were normalized against the signal we recorded in α-Quartz under the same experimental conditions. This latter crystal belongs to the 32 space group and thus exhibits the same nonlinear coefficients than [Fe(*phen*)$_3$](Δ-TRISCAS)$_2$ (**4**) and [Fe(*phen*)$_3$](Λ-TRISCAS)$_2$ (**5**) micro-crystallites under study. Moreover, the second-order optical susceptibility of α-Quartz is almost flat over the whole visible and near I.R spectral range. At variance with the SHS we recorded in α-Quartz, the SHS we recorded for either [Fe(*phen*)$_3$](Δ-

TRISCAS)$_2$ (**4**) or [Fe(*phen*)$_3$](Λ-TRISCAS)$_2$ (**5**) strongly increases as we tune the central wavelength of the laser pulses towards λ = 1050 nm. As previously mentioned, these two samples present a small and broad absorption peak centered at λ = 520 nm related to the d-d transition of iron(II) that overlaps with the more intense MLCT absorption band due to the phenanthroline ligand.
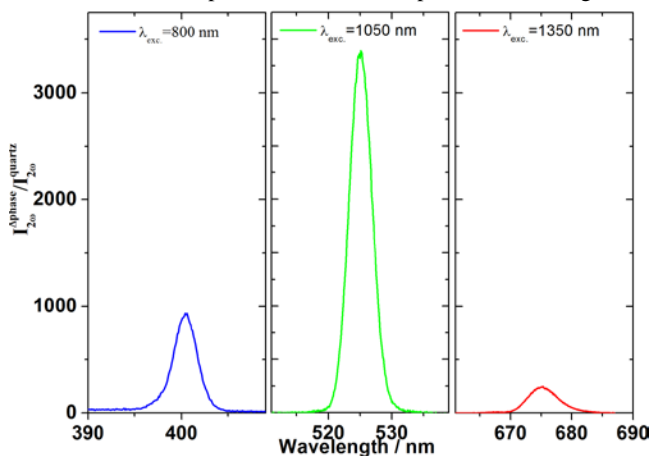

Figure 10: a) Spectra of the SHS recorded in [Fe(*phen*)$_3$](Δ-TRISCAS)$_2$ **4** under the same experimental condition when the excitation wavelength is centred at λ = 800 nm, 1050 nm and 1350 nm respectively. These signals are normalized against the signal recorded in α-Quartz under the same experimental conditions.

Hence the increase of the SHS when the excitation wavelength is about λ = 1050 nm is related to the resonant enhancement of the second-order susceptibility of this material. We published elsewhere extensive details about the experimental set-up, a more detailed study on films made of **7** and **8** of the SHG dependence on the irradiation wavelength, and the possibility of performing Sum Frequency Generation on two femtosecond laser pulses, a property with applications in nonlinear optics.[63] Overall complexes **4,5**, **7** and **8** present similar NLO characteristics. Indeed the behavior and the spectral dependence we have observed in the visible range is due to the MLCT transitions, which have similar intensities for all those complexes.

Conclusions

As initially desired, the use of a variety of chiral anions based on hexavalent P/As(V) (TRISCAT, TRISPHAT, TRISCAS) and tetravalent As(III) ([As$_2$(tartrate)$_2$]$^{2-}$) have allowed us to perform the chiral resolution of the well-known [Fe(*phen*)$_3$]$^{2+}$ complex. TRISCAS and a new lipophilic derivative of [As$_2$(tartrate)$_2$]$^{2-}$ we synthesized[93] allow easy resolutions by selective crystallization. We found that TRISCAS yields dichloromethane solvates that crystallize in the Sohncke space group *R*32 as inversion twins, with molar fractions reflecting the initial optical purity of the chiral anion. Recrystallization in acetonitrile yields the corresponding acetonitrile solvate which spontaneously resolve. Instead the [As$_2$(tartrate)$_2$]$^{2-}$ anion yields methanol/dichloromethane solvates that crystallize in the enantiomorphic *P*3$_1$21/*P*3$_2$21 space groups, even when starting from a racemic mixture of the chiral anion. With the chiral anion TRISPHAT, we observed racemization of the anion in solution which prevented the resolution of the complex.

Dichroic spectroscopic studies evidenced the racemization of the [Fe(*phen*)$_3$]$^{2+}$ complex in solution, while chiral induction was preserved in the solid state upon (re)crystallization. In order to study the second-order nonlinear optical properties, we tested also the

dropcasting of those complexes. We showed that using N,N-dimethylformamide solutions allow easy growth of good-quality films. Preservation of the chiral character of the complex was evidenced by very strong signals in second-harmonic generation experiments when irradiated with femtosecond laser pulses. Interestingly the second-harmonic signal intensity dependence with the excitation wavelength hinted at a resonant enhancement of the second-order susceptibility of this material. The [Fe(*phen*)$_3$]$^{2+}$ photophysics is presently very much studied, and we are now exploring the possibility of photoconverting the complex to its metastable HS state by ultrafast pumping, and then checking SHG in that transient state. Preliminary results show that it is a good candidate for an ultrafast switch for non-linear optics, and they will be reported elsewhere in due course.

ASSOCIATED CONTENT

Supporting information contains experimental details of anions and complexes synthesis and physical characterization: crystallographic data, electronic absorption, dichroic and NMR spectra, details on second-harmonic generation experiments, imaging, X-ray diffraction and Raman spectra of drop-casts films. This material is available free of charge via the Internet at http://pubs.acs.org.

AUTHOR INFORMATION

Corresponding Author

* P. R. : patrick.rosa@icmcb.cnrs.fr; E. F. : eric.freysz@u-bordeaux.fr

Present Addresses

(A.N.) COBRA UMR 6014 Bâtiment IRCOF - 1 Rue Tesniere - 76821 Mont St Aignan Cedex, France

(O.S.) Department of Chemistry, School of Science, The University of Tokyo, 7–3–1 Hongo, Bunkyo–ku, Tokyo 113–0033, Japan

(A.I.) Faculté des Sciences Appliquées, Département Aérospatiale et Mécanique, Université de Liège, Quartier Polytech 1 allée de la Découverte 9 4000 Liège 1 Belgium

Author Contributions

The manuscript was written through contributions of all authors.
Notes
† Died February 2017.
# See e.g structure DKSTBR in the CSD, where R,R-tartrates give a torsion angle between coordinated O atoms and the twofold axis bisecting the tartrates of +81.15° corresponding to the Λ enantiomer, while S,S-tartrates give -82.51°and the Δ enantiomer.
& We follow here the IUCr convention for spacegroups exempt of improper rotations, see e.g. http://reference.iucr.org/dictionary/Sohncke_groups

ACKNOWLEDGMENT

REFERENCES

(1) Zhang, W.; Alonso-Mori, R.; Bergmann, U.; Bressler, C.; Chollet, M.; Galler, A.; Gawelda, W.; Hadt, R. G.; Hartsock, R. W.; Kroll, T.; et al. Tracking Excited-State Charge and Spin Dynamics in Iron Coordination Complexes. *Nature* **2014**, *509* (7500), 345–348.

(2) Sousa, C.; De Graaf, C.; Rudavskyi, A.; Broer, R.; Tatchen, J.; Etinski, M.; Marian, C. M. Ultrafast Deactivation Mechanism of the Excited Singlet in the Light-Induced Spin Crossover of [Fe(2,2-Bipyridine)3]2+. *Chem. - A Eur. J.* **2013**, *19* (51), 17541–17551.

(3) Papai, M.; Vanko, G.; Graaf, C. De; Rozgonyi, T. Theoretical Investigation of the Electronic Structure of Fe (II) Complexes at Spin-State Transitions. *J. Chem. Theory Comput.* **2013**, *9*, 509–519.

(4) Vankó, G.; Bordage, A.; Pápai, M.; Haldrup, K.; Glatzel, P.; March, A. M.; Doumy, G.; Britz, A.; Galler, A.; Assefa, T.; et al. Detailed Characterization of a Nanosecond-Lived Excited State: X-Ray and Theoretical Investigation of the Quintet State in Photoexcited [Fe(Terpy)2]2+. *J. Phys. Chem. C* **2015**, *119* (11), 5888–5902.

(5) Tribollet, J.; Galle, G.; Jonusauskas, G.; Deldicque, D.; Tondusson, M.; Letard, J. F.; Freysz, E. Transient Absorption Spectroscopy of the Iron(II) [Fe(Phen)3]2+complex: Study of the Non-Radiative Relaxation of an Isolated Iron(II) Complex. *Chem. Phys. Lett.* **2011**, *513* (1–3), 42–47.

(6) Gallé, G.; Jonusauskas, G.; Tondusson, M.; Mauriac, C.; Letard, J. F.; Freysz, E. Transient Absorption Spectroscopy of the [Fe(2 CH3-Phen)3]2+complex: Study of the High Spin ↔ Low Spin Relaxation of an Isolated Iron(II) Complex. *Chem. Phys. Lett.* **2013**, *556*, 82–88.

(7) Létard, J.-F.; Guionneau, P.; Goux-Capes, L. Towards Spin Crossover Applications. *Top. Curr. Chem.* **2004**, *235* (Spin Crossover in Transition Metal Compounds III), 221–249.

(8) Monat, J. E.; McCusker, J. K. Femtosecond Excited-State Dynamics of an Iron(II) Polypyridyl Solar Cell Sensitizer Model. *J. Am. Chem. Soc.* **2000**, *122* (17), 4092–4097.

(9) Hauser, A. Ligand Field Theoretical Considerations. *Top. Curr. Chem.* **2004**, *233* (Spin Crossover in Transition Metal Compounds I), 49–58.

(10) Gütlich, P.; Goodwin, H. A. Spin Crossover—An Overall Perspective. *Top. Curr. Chem.* **2004**, *233* (Spin Crossover in Transition Metal Compounds I), 1–47.

(11) Decurtins, S.; Gütlich, P.; Köhler, C. P.; Spiering, H.; Hauser, A. Light-Induced Excited Spin State Trapping in a Transition-Metal Complex: The Hexa-1-Propyltetrazole-Iron (II) Tetrafluoroborate Spin-Crossover System. *Chem. Phys. Lett.* **1984**, *105* (1), 1–4.

(12) Hauser, A. Intersystem Crossing in the [Fe(Ptz)6](BF4)2 Spin Crossover System (Ptz= 1-propyltetrazole). *J. Chem. Phys.* **1991**, *95* (February), 2741–2748.

(13) Mcgarvey, J. J.; Lawthers, I. Charge-Transfer Absorption Band. *J. Chem. Soc. Chem. Commun.* **1982**, 906–907.

(14) Lemke, H. T.; Kjær, K. S.; Hartsock, R.; Van Driel, T. B.; Chollet, M.; Glownia, J. M.; Song, S.; Zhu, D.; Pace, E.; Matar, S. F.; et al. Coherent Structural Trapping through Wave Packet Dispersion during Photoinduced Spin State Switching. *Nat. Commun.* **2017**, *8* (May), 15342.

(15) Zerdane, S.; Wilbraham, L.; Cammarata, M.; Iasco, O.; Rivière, E.; Boillot, M.-L.; Ciofini, I.; Collet, E. Comparison of Structural Dynamics and Coherence of D–d and MLCT Light-Induced Spin State Trapping. *Chem. Sci.* **2017**, *8* (7), 4978–4986.

(16) Sousa, C.; Llunell, M.; Domingo, A.; de Graaf, C. Theoretical Evidence for the Direct 3 MLCT-HS Deactivation in the Light-Induced Spin Crossover of Fe(Ii)–polypyridyl Complexes. *Phys. Chem. Chem. Phys.* **2018**, *20* (4), 2351–2355.

(17) Field, R.; Liu, L. C.; Gawelda, W.; Lu, C.; Miller, R. J. D. Spectral Signatures of Ultrafast Spin Crossover in Single Crystal [FeII(Bpy)3](PF6)2. *Chem. - A Eur. J.* **2016**, *22* (15), 5118–5122.

(18) Auböck, G.; Chergui, M. Sub-50-Fs Photoinduced Spin Crossover in [Fe(Bpy)3]$^{2+}$. *Nat. Chem.* **2015**, *7* (8), 629–633.

(19) Brady, C.; McGarvey, J. J.; McCusker, J. K.; Toftlund, H.; Hendrickson, D. N. Time-Resolved Relaxation Studies of Spin Crossover Systems in Solution. *Top Curr Chem* **2004**, *235* (Spin Crossover in Transition Metal Compounds III), 1–22.

(20) Juban, E. A.; Smeigh, A. L.; Monat, J. E.; McCusker, J. K. Ultrafast Dynamics of Ligand-Field Excited States. *Coord. Chem. Rev.* **2006**, *250* (13–14), 1783–1791.

(21) Gawelda, W.; Pham, V. T.; Van Der Veen, R. M.; Grolimund, D.; Abela, R.; Chergui, M.; Bressler, C. Structural Analysis of Ultrafast Extended X-Ray Absorption Fine Structure with Subpicometer Spatial Resolution: Application to Spin Crossover Complexes. *J. Chem. Phys.* **2009**, *130* (12), 1–9.

(22) Gawelda, W.; Pham, V. T.; Benfatto, M.; Zaushitsyn, Y.; Kaiser, M.; Grolimund, D.; Johnson, S. L.; Abela, R.; Hauser, A.; Bressler, C.; et al. Structural Determination of a Short-Lived Excited Iron(II) Complex by Picosecond X-Ray Absorption Spectroscopy. *Phys. Rev. Lett.* **2007**, *98* (5), 6–9.

(23) Gawelda, W.; Cannizzo, A.; Pham, V.-T.; van Mourik, F.; Bressler, C.; Chergui, M. Ultrafast Nonadiabatic Dynamics of [Fe^{II}(Bpy)$_3$]$^{2+}$ in Solution. *J. Am. Chem. Soc.* **2007**, *129* (26), 8199–8206.

(24) Consani, C.; Prémont-Schwarz, M.; Elnahhas, A.; Bressler, C.; Van Mourik, F.; Cannizzo, A.; Chergui, M. Vibrational Coherences and Relaxation in the High-Spin State of Aqueous [FeIIbpy3]2. *Angew. Chemie - Int. Ed.* **2009**, *48* (39), 7184–7187.

(25) Bressler, C.; Milne, C.; Pham, V.-T.; ElNahhas, A.; Veen, R. M. van der; Gawelda, W.; Johnson, S.; Beaud, P.; Grolimund, D.; Kaiser, M.; et al. Femtosecond XANES Study of the Light-Induced Spin Crossover Dynamics in an Iron(II) Complex. *Science* **2009**, *323* (January), 489–492.

(26) Naim, A. Rational Design, Synthesis and Characterization of Chiral Spin Crossover Compounds, UNIVERSITÉ DE BORDEAUX, 2016.

(27) Senthil Kumar, K.; Ruben, M. Emerging Trends in Spin Crossover (SCO) Based Functional Materials and Devices. *Coord. Chem. Rev.* **2017**, *346*, 176–205.

(28) Hashibe, T.; Fujinami, T.; Furusho, D.; Matsumoto, N.; Sunatsuki, Y. Chiral Spin Crossover Iron(II) Complex, Fac-Λ-[FeII(HLR)3](ClO4)2· EtOH (HLR= 2-Methylimidazol-4-Yl-Methylideneamino-R-(+)-1- Methylphenyl). *Inorganica Chim. Acta* **2011**, *375* (1), 338–342.

(29) Wang, Q.; Venneri, S.; Zarrabi, N.; Wang, H.; Desplanches, C.; Létard, J.-F.; Seda, T.; Pilkington, M. Stereochemistry for Engineering Spin Crossover: Structures and Magnetic Properties of a Homochiral vs. Racemic [Fe(N 3 O 2)(CN) 2] Complex. *Dalt. Trans.* **2015**, *44* (15), 6711–6714.

(30) Burrows, K. E.; McGrath, S. E.; Kulmaczewski, R.; Cespedes, O.; Barrett, S. A.; Halcrow, M. A. Spin States of Homochiral and Heterochiral Isomers of [Fe(PyBox)2]2+ Derivatives. *Chem. - A Eur. J.* **2017**, *23* (38), 9067–9075.

(31) Acha, R. T.; Pilkington, M. Probing the Structural Changes Accompanying a Spin Crossover Transition in a Chiral [Fe(<scp>ii</Scp>)(N 3 O 2)(CN) 2] Macrocycle by X-Ray Crystallography. *CrystEngComm* **2015**, *17* (46), 8897–8905.

(32) Sekimoto, Y.; Karim, M. R.; Saigo, N.; Ohtani, R.; Nakamura, M.; Hayami, S. Crystal Structures and Spin-Crossover Behavior of Iron(II) Complexes with Chiral and Racemic Ligands. *Eur. J. Inorg. Chem.* **2017**, *2017* (7), 1048.

(33) Qin, L.-F.; Pang, C.-Y.; Han, W.-K.; Zhang, F.-L.; Tian, L.; Gu, Z.-G.; Ren, X.; Li, Z. Spin Crossover Properties of Enantiomers, Co-Enantiomers, Racemates, and Co-Racemates. *Dalt. Trans.* **2016**, *45* (17), 7340–7348.

(34) Bartual-Murgui, C.; Pineiro-López, L.; Valverde-Munoz, F. J.; Munoz, M. C.; Seredyuk, M.; Real, J. A. Chiral and Racemic Spin Crossover Polymorphs in a Family of Mononuclear Iron(II) Compounds. *Inorg. Chem.* **2017**, *56* (21), 13535–13546.

(35) Bonhommeau, S.; Lacroix, P. G.; Talaga, D.; Bousseksou, A.; Seredyuk, M.; Fritsky, I. O.; Rodriguez, V. Magnetism and Molecular Nonlinear Optical Second-Order Response Meet in a Spin Crossover Complex. *J. Phys. Chem. C* **2012**, *116* (20), 11251–11255.

(36) Cavezzan, J.; Etemao-Moghadam, G.; Koenig, M.; Klaebe, A. ISOMERISATION DE COMPOSES OU PHOSPHORE HEXACOORDINE OPTIQUEMENT ACTIFS : MISE EN EVIDENCE D'UN PROCESSUS IRREGULIER. *Tetrahedron Lett.* **1979**, No. 9, 795–798.

(37) Rosenheim, A.; Plato, W. Optically Active Tribenzene Catechol-Arsenic Acid S. *Chem. Ber.* **1925**, *58* (August), 2000–2009.

(38) Ryschkewitsch, G. E.; Garrett, J. M. Synthesis of Asymmetric Boron Cations and Resolution with As(C6H4O2)3- Anion. *J. Am. Chem. Soc.* **1968**, *90* (26), 7234–7238.

(39) Lacour, J.; Ginglinger, C.; Favarger, F. Asymmetric Recognition of TRISPHAT Anion. Unusually High Difference in Reactivity of the Pseudoenantiomers of Cinchona Alkaloids. *Tetrahedron Lett.* **1998**, *39* (27), 4825–4828.

(40) Favarger, F.; Goujon-ginglinger, C.; Monchaud, D.; Bozec, L.; Inorg, H. E. J. Large-Scale Synthesis and Resolution of [Tris (Tetrachlorobenzenediolato) Phosphate (V)] Anion Ure 1), First Identified by Allcock in the Crude Reaction Mixture of Tricyclic Hexachlorocyclotriphosphazene and Pyrocatechol , 10 Was Later Shown to Be S. **2004**, No. V, 8521–8524.

(41) Jodry, J. J.; Frantz, R.; Lacour, J. Supramolecular Stereocontrol of Octahedral Metal-Centered Chirality. Ligand Modulation. *Inorg. Chem.* **2004**, *43* (11), 3329–3331.

(42) Reddy G. N., M.; Ballesteros-Garrido, R.; Lacour, J.; Caldarelli, S. Determination of Labile Chiral Supramolecular Ion Pairs by Chromatographic NMR Spectroscopy. *Angew. Chemie - Int. Ed.* **2013**, *52* (11), 3255–3258.

(43) Jodry, J. J.; Lacour, J. Efficient Resolution of a Dinuclear Triple Helicate by Asymmetric Extraction/Precipitation with TRISPHAT Anions as Resolving Agents. *Chem. - A Eur. J.* **2000**, *6* (23), 4297–4304.

(44) Sénéchal-David, K.; Toupet, L.; Maury, O.; Le Bozec, H. Supramolecular Solid-State Interactions between Helicene-like Terpyridinium Cation and Tris(Tetrachloro-Benzenediolato)Phosphate(V) (TRISPHAT) Anion. *Cryst. Growth Des.* **2006**, *6* (6), 1493–1496.

(45) Lacour, J.; Jodry, J. J.; Ginglinger, C.; Torche-Haldimann, S. Diastereoselective Ion Pairing of TRISPHAT Anions and Tris(4,4'-Dimethyl-2,2'-Bipyridine)Iron(II). *Angew. Chemie - Int. Ed.* **1998**, *37* (17), 2379–2380.

(46) Bark, T.; Von Zelewsky, A.; Rappoport, D.; Neuburger, M.; Schaffner, S.; Lacour, J.; Jodry, J. Synthesis and Stereochemical Properties of Chiral Square Complexes of Iron(II). *Chem. - A Eur. J.* **2004**, *10* (19), 4839–4845.

(47) PÉROLLIER, C.; BERNARDINELLI, G.; LACOUR, J. Sugar Derived Hexacoordinated Phosphates: Chiral Anionic Auxiliaries with General Asymmetric Efficienc. *Chirality* **2008**, *20* (July), 313–324.

(48) Monchaud, D.; Jodry, J. J.; Pomeranc, D.; Heitz, V.; Chambron, J. C.; Sauvage, J. P.; Lacour, J. Ion-Pair-Mediated Asymmetric Synthesis of a Configurationally Stable Mononuclear Tris(Diimine)-Iron(II) Complex. *Angew. Chemie - Int. Ed.* **2002**, *41* (13), 2317–2319.

(49) Bott, R. C.; Smith, A. G.; Sagatys, B. D. S.; C, A. D. E. L.; D, C. H. L. K. Group 15 Complexes with α -Hydroxy Carboxylic Acids : 7 * The Preparation and Structure Determination of Sodium (+) -Tartrato Arsenate (III), [Na 8 As 10 (C 4 H 2 O 6) 8 (C 4 H 3 O 6) 2 (H 2 O) 19] N ; Silver (I) (+) - Tartrato Arsenate (. *Aust. J. Chem.* **2000**, *10* (November), 917–924.

(50) Palenik, R. C.; Abboud, K. A.; Palenik, G. J. Bond Valence Sums and Structural Studies of Antimony Complexes Containing Sb Bonded Only to O Ligands. *Inorganica Chim. Acta* **2005**, *358* (4), 1034–1040.

(51) Dwyer, F. P.; Gyarfas, E. C. The Resolution of the Tris o,Phenantroline Ferrous Ion and the Oxidation of the Enantiomorphous Forms. *J. Proc. R. Soc. New South Wales* **1949**, *83*, 263–265.

(52) Zalkin, A.; Templeton, D. H.; Ueki, T. Crystal Structure of L-Tris(1,10-Phenanthroline) Iron(II) Bis(Antomony(III)d-Tartrate) Octahydrate. *Inorg. Chem.* **1973**, *12* (7), 1641–1646.

(53) Watson, R. T.; Jackson, J. L.; Harper, J. D.; Kane-maguire, K. A.; Kane-maguire, L. A. P.; Kane-maguire, N. A. P. Cis-[Ru(Phen)2(CH3CN)2] 2 +. *Inorganica Chim. Acta* **1996**, *249*, 5–7.

(54) Koda, S. No Title. *J. Sci. Hiroshima Univ. A* **1987**, *51*, 113.

(55) Matsumoto, K.; Kawaguchi, H.; Kuroya, H.; Kawaguchi, S. The Crystal Structure of (-)589-Acetylacetonatobis(Trimethylenediamine)Cobalt(III) Arsenic(V) (+)-Tartrate Monohydrate. *Bull. Chem. Soc. Jpn.* **1973**, *46*, 2424–

2428.

(56) Sarma, B. Das; Bailar, J. C. The Stereochemistry of Complex Inorganic Compounds. XVIII. A New Method for the Preparation of Inorganic Complexes in Their Optically Active Forms. *J. Am. Chem. Soc.* **77**, 5480–5482.

(57) Sakaguchi, U.; Tomioka, K.; Takaki, K.; Yoneda, H. Structure , Thermal Racemization , and Ion Association of the [1,1,1-Tris(5a-Mino-2-Azapentyl)Ethane]Cobalt (III) Complex. *Inorg. Chem.* **1985**, *24*, 463–467.

(58) Yamazaki, S.; Yoneda, H. CHROMATOGRAPHIC STUDY OF OPTICAL RESOLUTION. IV. COMPLETE RESOLUTION OF THE NEUTRAL COMPLEX, MERIDIONAL ISOMER OF TRIS(B-ALANINATO)COBALT(III). *Inorg. Nucl. Chem. Lett.* **1979**, *15*, 195–197.

(59) Miyoshi, K.; Izumoto, S.; Nakai, K.; Yoneda, H. Mechanism of Chiral Recognition of Octahedral Metal Complexes Effected by Bis(Mu-d-Tartrato)Diantimonate(III) Anion in Solution. 2. Cage Complexes of the Type [Co(N)6]3+. *Inorg. Chem.* **1986**, *25*, 4654–4657.

(60) Miyoshi, K.; Izumoto, S.; Yoneda, H. Mechanism of Chiral Recognition of Octahedral Metal Complexes Effected by Bis(Mu-d-Tartrato)-Diantimonate(III) Anion in Solution. I. Association Models and Their Application to Some [Co(N)6]3+-Type Complexes. *Bull. Chem. Soc. Jpn.* **1986**, *59*, 3475–3482.

(61) IUPAC. Tentative Proposals for Nomenclature1 of Absolute Configurations Concerned with Six-Coordinated Complexes Based on the Octahedron. *Inorg. Chem.* **1970**, *9* (1), 1–5.

(62) IUPAC. BASIC TERMINOLOGY OF STEREOCHEMISTRY. *Pure Appl. Chem.* **1996**, *68* (July), 2193–2222.

(63) Iazzolino, A.; Hamouda, A. O.; Naïm, A.; Stefánczyk, O.; Rosa, P.; Freysz, E. Nonlinear Optical Properties and Application of a Chiral Spin Crossover Compound. *Appl. Phys. Lett.* **2017**, *110*, 161908.

(64) Ohkoshi, S. I.; Takano, S.; Imoto, K.; Yoshikiyo, M.; Namai, A.; Tokoro, H. 90-Degree Optical Switching of Output Second-Harmonic Light in Chiral Photomagnet. *Nat. Photonics* **2014**, *8* (1), 65–71.

(65) Lemus, L.; Guerrero, J.; Costamagna, J.; Lorca, R.; Jara, D. H.; Ferraudi, G.; Oliver, A.; Lappin, A. G. Resolution and Characterization of Helicate Dimer and Trimer Complexes of 1,3-Bis(9-Methyl-1,10-Phenanthrolin-2-Yl)Propane with Copper(I). *Dalt. Trans.* **2013**, *42* (32), 11426.

(66) Habermehl, N. C.; Angus, P. M.; Kilah, N. L.; Nore, L.; Rae, A. D.; Willis, A. C.; Wild, S. B. Asymmetric Transformation of a Double-Stranded , Dicopper (I) Helicate Containing Achiral Bis (Bidentate) Schiff Bases. *Inorg. Chem.* **2006**, *45* (4), 1445–1462.

(67) Flack, H. D. Absolute-Structure Determination: Past, Present and Future. *Chim. Int. J. Chem.* **2014**, *68* (1), 26–30.

(68) Flack, H. D.; Shmueli, U. The Mean-Square Friedel Intensity Difference in P1 with a Centrosymmetric Substructure. *Acta Crystallogr. Sect. A Found. Crystallogr.* **2007**, *63* (3), 257–265.

(69) Flack, H. D.; Bernardinelli, G. Applications and Properties of the Bijvoet Intensity Ratio. *Acta Crystallogr. Sect. A Found. Crystallogr.* **2008**, *64* (4), 484–493.

(70) Flack, H. D.; Bernardinelli, G. The Use of X-Ray Crystallography to Determine Absolute Configuratio. *Chirality* **2008**, *20*, 681–690.

(71) Shmueli, U.; Flack, H. D. Concise Intensity Statistics of Friedel Opposites and Classification of the Reflections. *Acta Crystallogr. Sect. A Found. Crystallogr.* **2009**, *65* (4), 322–325.

(72) Flack, H. D.; Sadki, M.; Thompson, A. L.; Watkin, D. J. Practical Applications of Averages and Differences of Friedel Opposites. *Acta Crystallogr. Sect. A Found. Crystallogr.* **2011**, *67* (1), 21–34.

(73) Parsons, S.; Pattison, P.; Flack, H. D. Analysing Friedel Averages and Differences. *Acta Crystallogr. Sect. A Found. Crystallogr.* **2012**, *68* (6), 736–749.

(74) Parsons, S.; Flack, H. D.; Wagner, T. Use of Intensity Quotients and Differences in Absolute Structure Refinement. *Acta Crystallogr. Sect. B Struct. Sci. Cryst. Eng. Mater.* **2013**, *69* (3), 249–259.

(75) Flack, H. D.; Bernardinelli, G.; Clemente, D. A.; Linden, A.; Spek, A. L. Centrosymmetric and Pseudo-Centrosymmetric Structures Refined as Non-Centrosymmetric. *Acta Crystallogr. Sect. B Struct. Sci.* **2006**, *62* (5), 695–701.

(76) Flack, H. D.; Bernardinelli, G. Centrosymmetric Crystal Structures Described as Non-Centrosymmetric: An Analysis of Reports in Inorganica Chimica Acta. *Inorganica Chim. Acta* **2006**, *359* (1), 383–387.

(77) Flack, H. D. Absolute-Structure Reports. *Acta Crystallogr. Sect. C Cryst. Struct. Commun.* **2013**, *69* (8), 803–807.

(78) Goodwin, H. A. Spin Crossover in Iron(II) Tris(Diimine) and Bis(Terimine) Systems. *Top. Curr. Chem.* **2004**, *233* (Spin Crossover in Transition Metal Compounds I), 59–90.

(79) Spek, A. L. PLATON SQUEEZE: A Tool for the Calculation of the Disordered Solvent Contribution to the Calculated Structure Factors. *Acta Crystallogr. Sect. C Struct. Chem.* **2015**, *71*, 9–18.

(80) Harada, N.; Nakanishi, K.; Berova, N.; Overview, H. Electronic CD Exciton Chirality Method: Principles and Applications. In *Comprehensive Chiroptical Spectroscopy*; Berova, N., Polavarapu, P. L., Nakanishi, K., Woody, R. W., Eds.; John, 2012; Vol. 2, pp 115–166.

(81) Kaizaki, S. Applications of Electronic Circular Dichroism to Inorganic Stereochemistry. In *Comprehensive Chiroptical Spectroscopy*; Berova, N., Polavarapu, P. L., Nakanishi, K., Woody, R. W., Eds.; John Wiley&Sons, 2012; Vol. 2, pp 451–471.

(82) Mason, J.; Mason, S. F. Electronic Absorption and Circular Dichroism Spectra and Absolute Stereochemistry of Tris-Catechyl-Arsenate(V) Ion. *Tetrahedron* **1967**, *23* (4), 1919-.

(83) Ito, T.; Kobayashi, A.; Narumo, F.; Saito, Y. The Absolute Configuration of (-)589-Tris(1,2-Benzene-Diolato)Arsenate(V) Ion, (-)589-[As(Cat)3]-. *Inorg.* **1971**, *7*, 1097–1102.

(84) BRIZARD, A.; BERTHIER, D.; AIMÉ, C.; BUFFETEAU, T.; CAVAGNAT, D.; DUCASSE, L.; HUC, I.; ODA, R. Molecular and Supramolecular Chirality in Gemini-Tartrate Amphiphiles Studied by Electronic and Vibrational Circular Dichroisms. *Chirality* **2009**, *21*, E153–E162.

(85) Zhang, Z.; Yao, S.; Li, Y.; Cle, R.; Lu, Y.; Su, Z.; Wang, E. Protein-Sized Chiral Fe 168 Cages with NbO-Type Topology H NMR (Figure S14 ; See Supporting Information). *J. Am. Chem. Soc.* **2009**, No. c, 14600–14601.

(86) Hoffmann, M.; Grajewski, J.; Gawronski, J. Extending the Applications of Circular Dichroism in Structure Elucidation: Aqueous Environment Breaks the Symmetry of Tartrate Dianion. *New J. Chem.* **2010**, *34* (9), 2020.

(87) McCaffery, A. J.; Mason, S. F.; Norman, B. J. Optical Rotatory Power of Co-Ordination Compounds. Part XII Spectroscopic and Configurational Assignments for the Tris-Bipyridyl and -Phenanthroline Complexes of the Di- and Tri-Valent Iron-Group Metal Loins. *J. Chem. Soc* **1969**, 1428–1441.

(88) Rzepa, H. S.; Cass, M. E. In Search of the Bailar and Ra ˆ y − Dutt Twist Mechanisms That Racemize Chiral Trischelates : A Computational Study of Sc III , Ti IV , Co III , Zn II , Ga III , and Ge IV Complexes of a Ligand Analogue of Acetylacetonate. *Inorg. Chem.* **2007**, *46*, 451–457.

(89) Kolp, B.; Viebrock, H.; von Zelewsky, A.; Abeln, D. Crystal Structure Analysis and Chiral Recognition Study of Δ-[Ru(Bpy) 2 (Py) 2][(+)- O , O '-Dibenzoyl- d -Tartrate]·12H 2 O and Λ-[Ru(Bpy) 2 (Py) 2][(−)- O , O '-Dibenzoyl- l -Tartrate]·12H 2 O. *Inorg. Chem.* **2001**, *40* (6), 1196–1198.

(90) Pazderski, L.; Pawlak, T.; Sitkowski, J.; Kozerski, L.; Edward Szłyk. 1H NMR Assignment Corrections and 1H, 13C, 15N NMR Coordination Shifts Structural Correlations in Fe(II), Ru(II) and Os(II) Cationic Complexes with 2,2-Bipyridine and 1,10-Phenanthroline. *Magn. Reson. Chem.* **2010**, *48* (6), 450–457.

(91) Kuroda, R. Chirality in Crystals. In *Engineering of Crystalline Materials Properties*; Novoa, J. J., Ed.; Springer, 2008; pp 251–270.

(92) Kuroda, R.; Harada, T.; Shindo, Y. A Solid-State Dedicated Circular Dichroism Spectrophotometer: Development and Application. *Rev. Sci. Instrum.* **2001**, *72* (10), 3802–3810.

(93) Srinivasan, A.; Cortijo, M.; Bulicanu, V.; Naim, A.; Clérac, R.; Sainctavit, P.; Rogalev, A.; Wilhelm, F.; Rosa, P.; Hillard, E. A. Enantiomeric Resolution and X-Ray Optical Activity of a Tricobalt Extended Metal Atom Chain. *Chem. Sci.* **2018**, *1*, 1136–

11

1143.
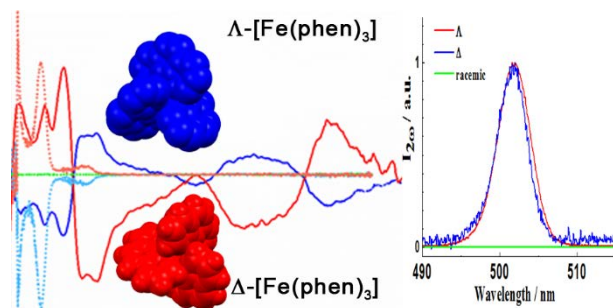
We report here the synthesis of [Fe(*phen*)$_3$]$^{2+}$ complexes resolved with chiral anions . Complexes containing TRISCAT and TRISCAS anions crystallize as inversion twins in the Sohncke *R*32 space group. Arsenyl tartrate anions yield structures in enantiomorphic *P*3$_1$21/*P*3$_2$21 space groups. Those molecular materials can be easily drop-cast as films, and NLO studies of the TRISCAS complex revealed very strong second-harmonic generation correlated with the electronic spectrum and its dichroic counterpart.